

# Single-Wall Carbon Nanotube Films

T. V. Sreekumar, Tao Liu, and Satish Kumar\*

*School of Textile and Fiber Engineering, Georgia Institute of Technology,  
Atlanta, Georgia 30332*

Lars M. Ericson, Robert H. Hauge, and Richard E. Smalley

*Department of Chemistry, Rice University, Houston, Texas 77005*

*Received April 4, 2002. Revised Manuscript Received October 15, 2002*

An optically homogeneous solution/dispersion of single-wall carbon nanotubes (SWNTs) in oleum has been used to form isotropic films exhibiting fibrillar morphology. Tensile modulus, strength, and strain to failure of the film are 8 GPa, 30 MPa, and 0.5%, respectively. The electrical conductivity in the plane of the film is  $1 \times 10^5$  S/m.

## Introduction

Single-wall carbon nanotubes (SWNT) have been the subject of intense research since their discovery<sup>1,2</sup> due to their high aspect ratio, Young's modulus, tensile strength, low density, and electrical properties.<sup>3–6</sup> However, it has been difficult to explore the full potential of these materials due to their insolubility at reasonable concentrations in common solvents.<sup>7</sup> Attempts have been reported to dissolve and characterize SWNTs in various organic solvents such as dimethyl formamide (DMF) and *N*-methyl pyrrolidone.<sup>8</sup> It has been shown that SWNTs whose lengths have been reduced by sonication (in the range of 100–300 nm)<sup>9</sup> can be rendered soluble in common organic solvents by covalent functionalization.<sup>7</sup> Dissolution of full-length SWNTs by one-step exfoliation and noncovalent (ionic) functionalization of the carboxylic acid groups present in the purified SWNTs has also been reported.<sup>10</sup>

Fabrication of macroscopic nanotube products such as films and fibers for practical applications is a major challenge. A number of attempts to form such macroscopic products have recently been reported.<sup>11,12</sup> Here, we report SWNT film formation from optically transparent and nonbirefringent SWNT solution in oleum-

containing 30% sulfur trioxide. Thermal, mechanical, and electrical properties of the films have been characterized.

## Experimental Section

Single-wall carbon nanotubes used in this study were produced using the HiPCO process.<sup>13,14</sup> The purified tubes<sup>15</sup> were vacuum-dried at 110 °C. Thermogravimetric analysis of these purified tubes in air exhibited 7 wt % residue above 800 °C, suggesting the presence of significant catalytic impurity even after purification. Vacuum-dried purified SWNTs (0.125 g) were mixed in 50 g of oleum (H<sub>2</sub>SO<sub>4</sub>:30%SO<sub>3</sub>) in a glass flask placed in a glovebox. The solution was stirred using a magnetic stirrer and maintained at 60 °C. Dry nitrogen gas flow was maintained in the glovebox.

A small amount of SWNT/oleum solution/dispersion was poured into a dry Petri dish in the glovebox. The covered Petri dish was then taken out of the glovebox and kept in the hood and the Petri dish cover was removed. As the solution absorbed moisture from the room temperature air, acid began to leach out. Once all the acid was leached out and removed from the Petri dish, the resulting film was washed with acetone and then with distilled water to remove the remaining acid. The film was finally washed with acetone and dried at 110 °C for 1 h and subsequently heat-treated at 350 °C under a nitrogen atmosphere for 1 h. These films are referred to as as-prepared (vacuum dried at 110 °C) and heat-treated (at 350 °C) films, respectively.

For SEM study, films were fractured at room temperature and mounted on an aluminum stub using a conducting tape and were observed in a LEO 1530 scanning electron microscope without applying any conducting coating. Thermogravimetric studies were performed at 10 °C/min in nitrogen on TA Instruments TGA2950. The Raman spectra were collected using a Holoprobe Research 785 Raman Microscope made by Kaiser Optical System, Inc. with a laser wavelength of 785

\* To whom correspondence should be addressed. E-mail: satish.kumar@textiles.gatech.edu.

- (1) Iijima, S.; Ichihashi, T. *Nature* **1993**, *363*, 603.
- (2) Bethune, D. S.; Kiang, C. H.; de Vries, M. S.; Gorman, G.; Savoy, R.; Vazquez, B.; Beyers, R. *Nature* **1993**, *363*, 605.
- (3) Saito, R.; Dresselhaus, G.; Dresselhaus, M. S. *Physical Properties of Carbon Nanotubes*; Imperial College Press: London, 1998.
- (4) Yu, M. F.; Files, B. S.; Arepalli, S.; Ruoff, R. S. *Phys. Rev. Lett.* **2000**, *84*, 5552.
- (5) Lu, J. P. *Phys. Rev. Lett.* **1997**, *79*, 1297.
- (6) Yakobson, B. I.; Smalley, R. E. *Science* **1997**, *85*, 324.
- (7) Chen, J.; Hamon, M. A.; Hu, H.; Chen, Y.; Rao, A. M.; Ecklund, P. C.; Haddon, R. C. *Science* **1998**, *282*, 95.
- (8) Ausman, K. D.; Piner, R.; Lourie, O.; Ruoff, R. S.; Korobov, M. *J. phys. chem. B* **2000**, *104* (38), 8911.
- (9) Liu, J.; Rinzler, A. G.; Dai, H.; Hafner, J. H.; Bradley, R. K.; Boul, P. J.; Lu, A.; Iverson, T.; Shelimov, K.; Huffman, C. B.; Rodriguez-Macias, F.; Shon, Y.-S.; Lee, T. R.; Colbert, D. T.; Smalley, R. E. *Science* **1998**, *280*, 1253.
- (10) Chen, J.; Rao, A. M.; Lyuksyutov, S.; Itkis, M. E.; Hamon, M. A.; Hu, H.; Cohn, R. W.; Ecklund, P. C.; Colbert, D. T.; Smalley, R. E.; Haddon, R. C. *J. Phys. Chem. B* **2001**, *105*, 2525.

- (11) Vigolo, B.; Penicaud, A.; Coulon, C.; Sauder, C.; Pailler, R.; Journet, C.; Bernier, P.; Poulin, P. *Science* **2000**, *290*, 1331.

- (12) Li, Y. H.; Xu, C.; Wei, B.; Zhang, X.; Zheng, M.; Wu, D.; Ajayan, P. M. *Chem. Mater.* **2002**, *14*, 483.

- (13) Nikolaev, P.; Bronikowski, M. J.; Bradley, R. K.; Rohmund, F.; Colbert, D. T.; Smith, K. A.; Smalley, R. E.; *Chem. Phys. Lett.* **1999**, *313*, 91.

- (14) Bronikowski, M. J.; Willis P. A.; Colbert, D. T.; Smith, K. A.; Smalley, R. E. *J. Vac. Sci. Technol.* **2001**, *19*, 1800.

- (15) Chiang, I. W.; Brinson, B. E.; Smalley, R. E.; Margrave, J. L.; Hauge, R. H. *J. Phys. Chem. B* **2001**, *105*, 1157.

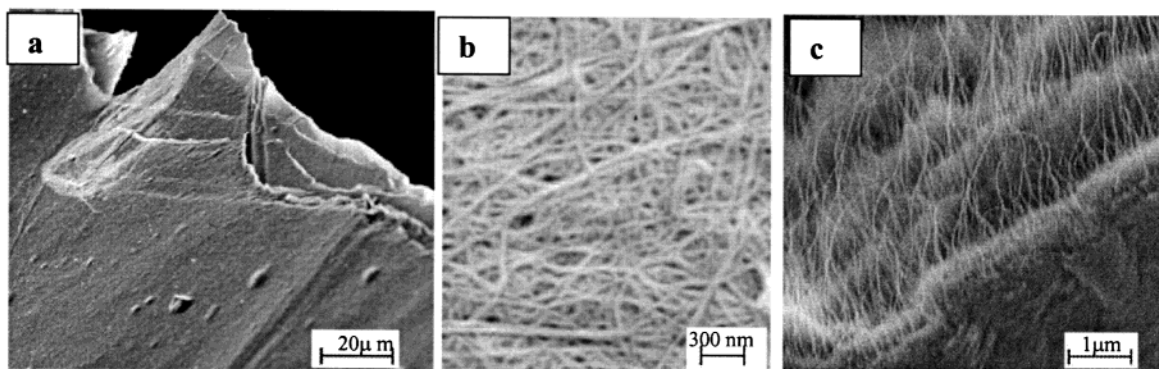


**Figure 1.** Scanning electron micrographs of the SWNT film.

**Table 1. Properties of SWNT and SWNT Films**

	electrical conductivity (S/m)	Raman peak position ( $\text{cm}^{-1}$ )	relative elemental composition (C:O:S:H)
purified SWNT powder	not measured	1591	97:3:0:0
as-prepared SWNT film	$1.3 \times 10^5$ (in the plane of the film)	1597	85.5:10.5:2.5:1.5
heat-treated SWNT film	$0.9 \times 10^5$ (in the plane of the film)	1593	89.6:9.9:0:0.5

nm. X-ray photoelectron spectroscopy (XPS) studies on SWNT and their films were carried out using a Surface Science SSX-100 ESCA spectrometer with monochromatic Al K $\alpha$  X-rays ( $h\nu = 1486.6$  eV). XPS curve-fitting routine defaults to 80% Gaussian/20% Lorentzian. Default backgrounds are fitted with the Shirley routine. Tensile tests were conducted on Rheometrics RSA III at a strain rate of 0.72%/min. For tensile tests, heat-treated film with a cross-sectional area of  $0.2 \times 0.0015$  cm and a gage length of 2.5 cm was used. Electrical conductivity was measured using the four-probe method. Film density was estimated by the flotation method using a 2-propanol and water mixture.

## Results and Discussion

Optical microscopy showed no nanotube aggregation and micrographs taken under cross-polarization showed no birefringence, suggesting an isotropic solution/dispersion. This solution/dispersion was stable for months at room temperature while kept in the glovebox with flowing nitrogen. The films made from this solution when observed at low magnification (Figure 1a) appear to be fairly smooth (i.e., no ropes or fibrils could be observed at this magnification); however, at high magnification, a fibrillar (or ropelike) character is clearly seen on the film surface (Figure 1b) as well as on the edge of the film (Figure 1c). The fibril/rope diameter is about 40 nm. There is no preferential orientation in the film plane. The SWNT isotropy in the film plane was also confirmed by polarized Raman spectroscopy.

Properties of purified SWNT powder, as-prepared SWNT film, and the heat-treated SWNT film are given in Table 1. The in-plane conductivity of the as-prepared and heat-treated films measured by the four-probe method at room temperature are  $1.3 \times 10^5$  and  $9.0 \times 10^4$  S/m, respectively. Compared to the conductivity parallel to the tube axis of individual SWNT rope<sup>16</sup> of  $1.0 \times 10^6$  to  $3.0 \times 10^6$  S/m, the in-plane conductivity of the as-prepared and heat-treated SWNT films is about 1 order of magnitude lower. However, compared to the bulk conductivity of a SWNT mat (bucky paper),<sup>16–19</sup>

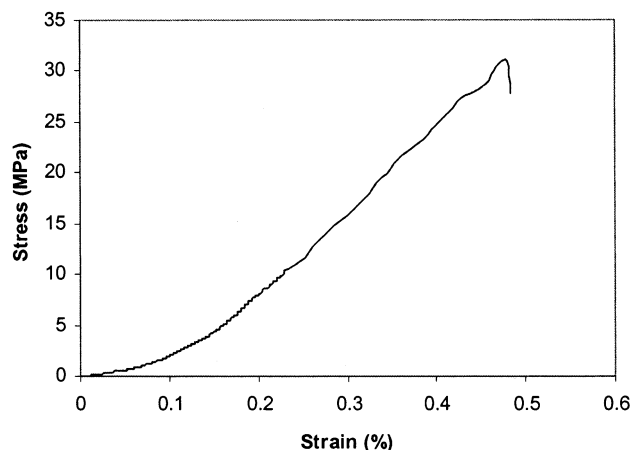


**Figure 2.** Stress–strain curve of heat-treated SWNT film.

which has a conductivity of  $2 \times 10^4$  to  $4 \times 10^4$  S/m, both the as-prepared and the heat-treated SWNT films have a much higher in-plane conductivity. The studies of pressure-dependent electrical conductivity of a SWNT mat<sup>17</sup> suggests that contact between ropes can be enhanced by applying a moderate pressure (10 kbar). Thus, the electrical conductivity of the SWNT mat increased from  $2.0 \times 10^4$  S/m at atmospheric pressure to  $1.0 \times 10^5$  S/m at 10 kbar. The difference between the electrical conductivities of SWNT film reported in this paper and SWNT mat reported in the literature may suggest a more densified structure for the former.

The tensile stress–strain curve of the heat-treated SWNT film is given in Figure 2. The tensile modulus, strength, and elongation to break values for the film are 8 GPa (at 0.2% strain), 30 MPa, and 0.5%, respectively. This would suggest that failure occurred via interfibrillar slippage rather than fracture within a fibril. Weight loss as a function of temperature in nitrogen is shown in Figure 3. Both the as-prepared and heat-treated SWNT films contain about 9 wt % oxygen, while oxygen content in the purified SWNT was about

(16) Fischer, J. E.; Dai, H.; A. Thess, R. L.; Hanjani, N. M.; Dehaas, D. L.; Smalley, R. E. *Phys. Rev. B* **1997**, *55*, 4921.

(17) Bozhko, A. D.; Sklovsky, D. E.; Nalimova, V. A.; Rinzler, A. G.; Smalley, R. E.; Fischer, J. E. *Appl. Phys. A* **1998**, *67*, 75.

(18) Kim, G. T.; Choi, E. S.; Kim, D. C.; Suh, D. S.; Park, Y. W.; Liu, K.; Duesberg G.; Roth, S. *Phys. Rev. B* **1998**, *58*, 16064.

(19) Kaiser, A. B.; Duesberg, G.; Roth, S. *Phys. Rev. B* **1998**, *57*, 1418.

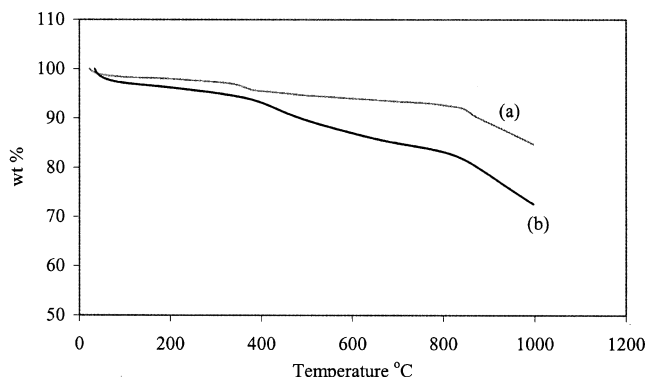


**Figure 3.** Thermogravimetric analysis of (a) purified SWNT powder and (b) heat-treated SWNT film in nitrogen.

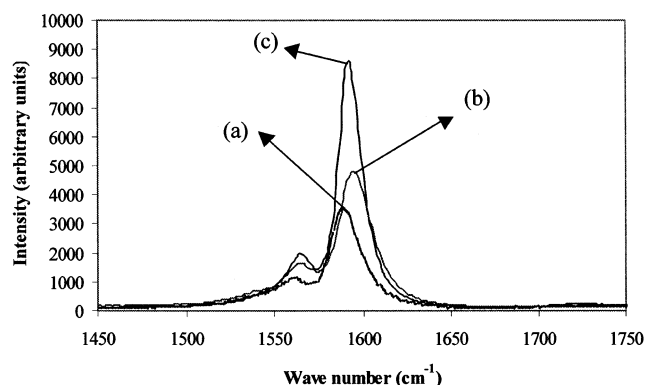


**Figure 4.** Raman spectra of (a) purified SWNT powder, (b) as-prepared SWNT film, and (c) heat-treated SWNT film using a laser excitation wavelength of 785 nm.

3 wt %. The difference in weight loss between the SWNTs and the SWNT film is attributed to the presence of excess oxygen in the film as well as to the presence of any traces of bisulfate ions and/or to the excess sulfuric acid. Film density was estimated to be about 0.9 g/cm<sup>3</sup>.

Raman spectra of purified SWNT powder, as well as that for the as-prepared and heat-treated SWNT films, are given in Figure 4. Raman peak for the strongest tangential stretching mode upshifts from 1591 cm<sup>-1</sup> for the neat SWNT to 1597 cm<sup>-1</sup> for the as-prepared SWNT film. Electrochemical oxidation<sup>20</sup> of SWNT in sulfuric acid suggests that a spontaneous charge transfer from SWNTs to sulfuric acid can result in a p-doped SWNT/sulfuric acid intercalated compound. Oleum, which is used in the present study, is a stronger oxidizing agent than the 95% H<sub>2</sub>SO<sub>4</sub> and may facilitate electron transfer more easily and oxidize the nanotubes. The residual positive charge on the nanotubes will lead to strong columbic repulsion, overcoming the van der Waals attraction within the nanotube rope, leading to dissolution. Nanotube dissolution did not occur in sulfur trioxide (SO<sub>3</sub>) as no bisulfate ions could be formed, and the charge transfer from the nanotube was hindered. The SWNT dissolution mechanism in oleum and other strong acids has been addressed elsewhere.<sup>21</sup>

The charge-transfer-induced C–C bond contraction stiffens the vibration of the tangential stretching mode

to cause a frequency upshift. Frequencies downshift due to the softening of the tangential stretching mode was also observed for n-doped (e.g., K, Rb) SWNTs.<sup>22,23</sup> The 6-cm<sup>-1</sup> frequency upshift in Raman peak position in as-prepared SWNT film as compared to that in purified SWNT powder is due to the positive charge on the nanotubes produced by the spontaneous charge transfer reaction with the residual sulfuric acid. These positive charges are reportedly stabilized by the bisulfate ions.<sup>20</sup> Upon heat treatment at 350 °C, the tangential stretching mode of the film recovered to 1593 cm<sup>-1</sup>. The 2-cm<sup>-1</sup> frequency difference between the purified SWNT powder and the heat-treated SWNT film may be attributed to the heating affect differences between the two samples,<sup>24–26</sup> as well as to the presence of residual dopant.

The Raman intensity decreases with the intercalation and increases with increased exfoliation and/or reduced van der Waals interactions. Sidewall chemistry or functionalization during the cleaning process can also affect Raman intensity. Extensive studies also show that, with increased applied pressure, the Raman scattering intensity of SWNT decreases due to the hexagonal distortion of the individual SWNT tubes.<sup>27–32</sup> SWNTs have a resonant enhanced Raman scattering effect due to its unique paired singular electronic density of states (Van Hove singularities).<sup>33–35</sup> In the Raman scattering process of SWNTs, when the incident or scattered photon energy matches the energy separation between any of these paired Van Hove singularities, very strong interband optical transition occurs, resulting in exceptionally high Raman scattering intensity. Depletion of the valance subband (p-doped SWNTs) or the filling of the conduction subband (n-doped SWNTs) results in depressing the optical transition between these paired Van Hove singularities.<sup>36–38</sup> However, on heat treatment to 350 °C, the dopant effect is minimized or eliminated, resulting in stronger Raman scattering

(22) Claye, A.; Rahman, S.; Fischer, J. E.; Sirenko, A.; Sumanasekera, G. U.; Eklund, P. C. *Chem. Phys. Lett.* **2001**, *333*, 16.

(23) Rao, A. M.; Eklund, P. C.; Bandow, S. J.; Thess, A.; Smalley, R. E. *Science* **1997**, *388*, 257.

(24) Zhang, L.; Li, H. D.; Yue, K. T.; Zhang, S. L.; Wu, X. H.; Zi, J.; Shi, Z. J.; Gu, Z. N. *Phys. Rev. B* **2002**, *65*, 073401.

(25) Huang, F. M.; Yue, K. T.; Tang, P. H.; Zhang, S. L.; Shi, Z. J.; Zhou, X. H.; Gu, Z. N. *J. Appl. Phys.* **1998**, *84*, 4022.

(26) Li, H. D.; Yue, K. T.; Lian, Z. L.; Zhan, Y.; Zhou, L. X.; Zhang, S. L.; Shi, Z. J.; Gu, Z. N.; Liu, B. B.; Yang, R. S.; Yang, H. B.; Zou, G. T.; Zhang, Y.; Iijima, S. *Appl. Phys. Lett.* **2000**, *76*, 2053.

(27) Venkateswaran, U. D.; Brandsen, E. A.; Schlecht, U.; Rao, A. M.; Richter, E.; Loa, I.; Syassen, K.; Eklund, P. C. *Phys. Status Solidi B* **2001**, *223*, 225.

(28) Teredesai, P. V.; Sood, A. K.; Sharma, S. M.; Karmakar, S.; Sikka, S. K.; Govindaraj, A.; Rao, C. N. R. *Phys. Status Solidi B* **2001**, *223*, 479.

(29) Venkateswaran, U. D.; Rao, A. M.; Richter, E.; Menon, M.; Rinzler, A.; Smalley, R. E.; Eklund, P. C. *Phys. Rev. B* **1999**, *59*, 10928.

(30) Teredesai, P. V.; Sood, A. K.; Muthu, D. V. S.; Sen, R.; Govindaraj, A.; Rao, C. N. R. *Chem. Phys. Lett.* **2000**, *319*, 296.

(31) Thomsen, C.; Reich, S.; Jantoljak, H.; Loa, I.; Syassen, K.; Burghard, M.; Duesberg, G. S.; Roth, S. *Appl. Phys. A* **1999**, *69*, 309.

(32) Sood, A. K.; Teredesai, P. V.; Muthu, D. V. S.; Sen, R.; Govindaraj, A.; Rao, C. N. R. *Phys. Status Solidi B* **1999**, *215*, 393.

(33) Dresselhaus M. S.; Eklund, P. C. *Adv. Phys.* **2000**, *49*, 705.

(34) Saito, R.; Dresselhaus, G.; Dresselhaus, M. S. *Phys. Rev. B* **2000**, *61*, 2981.

(35) Charlier, J. C.; Lambin, Ph. *Phys. Rev. B* **1998**, *57*, R15037.

(36) Kazaoui, S.; Minami, N.; Kataura, H.; Achiba, Y. *Synth. Met.* **2001**, *121*, 1201.

(37) Jacquemin, R.; Kazaoui, S.; Yu, D.; Hassanien, A.; Minami, N.; Kataura, H.; Achiba, Y. *Synth. Met.* **2000**, *115*, 283.

(38) Kazaoui, S.; Minami, N.; Jacquemin, R.; Katarua H.; Achiba, Y. *Phys. Rev. B* **1999**, *60*, 13339.

(20) Sumanasekera, G. U.; Allen, J. L.; Fang, S. L.; Loper, A. L.; Rao, A. M.; Eklund, P. C. *J. Phys. Chem. B* **1999**, *103*, 4292.

(21) Smalley, R. E. et al., to be submitted.



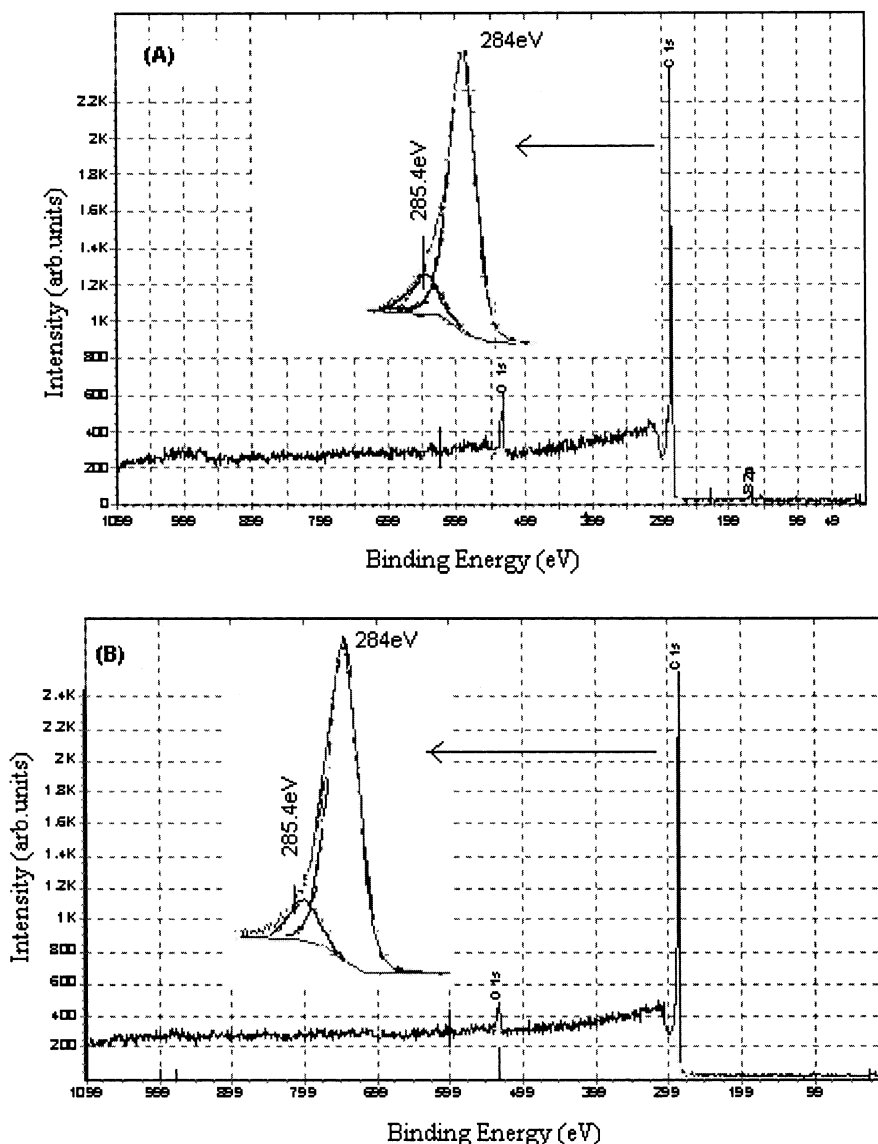


**Figure 5.** XPS of (a) as-prepared SWNT film and (b) purified SWNT powder.

intensity for the heat-treated SWNT film than that for the as-prepared film (Figure 4). The higher Raman scattering intensity of the as-prepared SWNT film as compared to that of the purified SWNT powder may be a result of competition between exfoliation and doping, both resulting from Oleum.

XPS shows that the as-received purified SWNT powder contains carbon and oxygen in the ratio of 97:3. Elemental analysis showed that the carbon, oxygen, sulfur, and hydrogen ratios in the as-prepared and heat-treated films were 85.5:10.5:2.5:1.5 and 89.6:9.9:0.0:0.5, respectively. The presence of about 1.5% hydrogen in the as-prepared film is consistent with the presence of bisulfate ions. While elemental analysis did not reveal the presence of sulfur in the heat-treated film, XPS did show the presence of sulfur. The XPS spectra of the as-received SWNTs and for the as-prepared SWNT films are shown in Figure 5. The insets in Figure 5 are the curve-fitted C 1s spectra, which show a main peak at 284 eV, corresponding to the  $sp^2$ -hybridized carbon, and a second carbon peak at 285.4 eV. Carbon at 284 eV is attributed to graphitic carbon, and in the range of 285–290 eV, it has been attributed to variously bonded carbons including C–OH, C=O, and COOH.<sup>39</sup>

## Conclusions

Optically isotropic SWNT solution/dispersion in Oleum has been used to cast SWNT film. The electrical conductivity of these films is about an order of magnitude higher than that for the SWNT mat (or the bucky paper). The differences in the Raman scattering intensity of the purified SWNT powder, as-prepared SWNT film, and the heat-treated SWNT film have been interpreted in terms of SWNT intercalation and doping resulting from Oleum.

**Acknowledgment.** We are thankful to Professor Brent Carter for XPS and to Dr. Runqing Ou for assistance in electrical conductivity measurement. Financial support for this work from AFOSR, ONR, Carbon Nanotechnologies Inc., and support at Rice University in developing the HiPco process from NASA, the Office of Naval Research, the Texas Advanced Technology Program, and the Robert A Welch Foundation is gratefully acknowledged.

CM020367Y

(39) Visvanathan, H.; Rooke, M. A.; Sherwood, P. M. A. *Surf. Interface Anal.* **1997**, *25*, 409.